Est. 1984

ORIENTAL JOURNAL OF CHEMISTRY
An International Open Access, Peer Reviewed Research Journal

www.orientjchem.org

ISSN: 0970-020 X
CODEN: OJCHEG
2019, Vol. 35, No.(3):
Pg. 958-965

Preparation of Stereocomplex Polylactide/poly(butylene succinate) Blends by Melt Blending

JENJIRA JIRUM and YODTHONG BAIMARK*

Biodegradable Polymers Research Unit, Department of Chemistry, Faculty of Science,
Mahasarakham University, Mahasarakham 44150, Thailand.
*Corresponding author E-mail: yodthong.b@msu.ac.th

http://dx.doi.org/10.13005/ojc/350306

(Received: November 23, 2018; Accepted: May 11, 2019)

ABSTRACT

Biodegradable polymer blends based on stereocomplex polylactide (scPLA) and poly(butylene succinate) (PBS) were successfully formed by continuous two-step melt blending. An epoxy-based, multifunctional chain extender was chosen to enhance phase compatibility of the blends. Effects of PBS and chain extender on thermal, phase morphology, thermo-mechanical and tensile properties of the scPLA/PBS blends were determined. The PBS blending enhanced plasticizing effect and cold-crystallization of scPLA matrix in an amorphous region. The chain-extension reaction inhibited crystallization of PBS, PLA homo-crystallites and PLA stereocomplex-crystallites as well as reduced thermal stability of the scPLA/PBS blends because of formation of long-chain branched structures. It has been shown that the poor phase compatibility between continuous scPLA and dispersed PBS phases of the blends may be solved through melt blending with a chain extender. The chain extension of scPLA/PBS blends also improved thermo-mechanical properties and flexibility of the scPLA/PBS blend films.

Keywords: Polylactide, Stereocomplex, Poly(butylene succinate), Polymer blends, Chain extender, Thermal properties.

INTRODUCTION

Poly(L-lactide) (PLLA) bioplastics have extensively investigated because of its biodegradability, renewability, good processability and low toxicity.[1–4] High-performance bioplastics of enantiomeric PLLA/poly(D-lactide) (PDLA) blends called as stereocomplex polylactides (scPLA) have been extensively reported.[5-7] The scPLA exhibited higher mechanical properties, better heat-resistance, faster crystallization rate and slower hydrolysis than the PLLA.[8-10] This is due to the scPLA had stronger intermolecular forces between PLLA and PDLA chains.[8,11]

The PLLA has been melt-blended with a flexible poly(butylene succinate) (PBS) to enhance flexibility and toughness as well as maintain complete biodegradability.[12-16] The PBS could form a miscible blend with PLLA in the amorphous region and enhanced the crystallization of PLLA matrix. However, scPLA/PBS blends have not been reported so far.

Joncryl® have been used as effective chain-extenders for producing long-chain branching PLLA during melt process to maintain its molecular weight.[17-19] However the effect of chain extender on properties of scPLA/PBS blends have not been published. Therefore the influences of PBS and chain extender on stereocomplexation and properties of scPLA was determined and discussed in this work.

EXPERIMENTAL

Materials

PLLA and PDLA were polymerized from L-lactide and D-lactide monomers, respectively.[20] 1-Dodecanol (98%, Fluka, Switzerland) and stannous octoate (95%, Sigma-Aldrich, Switzerland) were used as an initiator and a catalyst, respectively. Polymerization temperature and time were 165°C and 2.5 h respectively. PBS was kindly supplied by Multibax Public Co., Ltd., Thailand. PLLA, PDLA and PBS were characterized by a melt flow indexer (Tinius Olsen MP1200), polarimeter (Bellingham and Stanley ADP220) and differential scanning calorimeter (DSC, Perkin-Elmer Pyris Diamond). The properties of PLLA, PDLA and PBS are reported in Table 1. Joncryl® chain extender (ADR 4368, BASF, Thailand) was used as received. All reagents used were analytical grade.

Table 1: Properties of PLLA, PDLA and PBS

Sample	L-enantiomer content[a] (%)	MFI[b] (g/10 min)	T_g[c] (°C)	T_m[c] (°C)
PLLA	96.4	21	54	173
PDLA	3.2	24	59	176
PBS	-	30	-35	114

Preparation of scPLA/PBS blends

PLLA, PDLA, PBS and chain extender were blended at 200°C with 100 rpm rotor-speed using a Rheomix Haake internal mixer after drying at 50°C under vacuum overnight. The PLLA, PBS and chain extender were first melt blended for 10 min (step 1), then PDLA and remaining chain extender was added, and the blending was continued for 4 min (step 2). The 50% of 4.0 phr chain extender was added at each step of melt blending. The PLLA/PDLA weight ratio of scPLAs was 50/50. Effects of scPLA/PBS weight ratios (100/0, 95/5 and 90/10) and chain-extender addition (4.0 phr) on blend properties were investigated.

The scPLA/PBS blend films were fabricated using an Auto CH Caver compression molding machine at 240°C for 1.0 min without any force before compression with 5 ton force for 1.0 min. The obtained film was then cooled to room temperature. The films with 0.2–0.3 mm in thickness were obtained.

Characterization of scPLA/PBS blends

The DSC was used to determined thermal transitions of scPLA/PBS blends. The blend was melted at 250°C for 2 min to eliminate its thermal history before quenching to 0°C and then re-heated to 250°C. The heating rate was 10°C/minute.

The thermal decomposition behavior of the scPLA/PBS blends was measured with a TA-Instrument SDT Q600 thermogravimetric analyzer (TGA). The blends were heated from 50 to 600°C at the heating rate of 20°C/min under a N_2 flow.

Wide-angle X-ray diffraction (XRD) was used to measure crystalline characteristics of blend films using a Bruker D8 Advance XRD at 40 kV and 40 mA with CuKα radiation and 3°/min scan speed. Degrees of crystallinity (X_c) for homo-PLA (PLA-$X_{c,hc}$), stereocomplex-PLA (PLA-$X_{c,sc}$) and PBS (PBS-X_c) crystallites were calculated from equations (1)–(3), respectively.

$$\text{PBS-}X_c\ (\%) = [A_{c,PBS}/(A_{hc,PLA} + A_{sc,PLA} + A_{c,PBS} + Aa)] \times 100 \quad (1)$$

$$\text{PLA-}X_{c,hc}\ (\%) = [A_{hc,PLA}/(A_{hc,PLA} + A_{sc,PLA} + A_{c,PBS} + Aa)] \times 100 \quad (2)$$

$$\text{PLA-}X_{c,sc}\ (\%) = [A_{sc,PLA}/(A_{hc,PLA} + A_{sc,PLA} + A_{c,PBS} + Aa)] \times 100 \quad (3)$$

Where $A_{hc,PLA}$, $A_{sc,PLA}$, $A_{c,PBS}$ and A_a are the integrated intensity peaks for homo-PLA crystallites, stereocomplex-PLA crystallites and PBS crystallites as well as the integrated intensity of the amorphous halo, respectively.

Dynamic mechanical analyzer (DMA, Q800 TA Instruments) was used to determined thermo-mechanical properties of the blend films. The film with 5 × 20 × 0.2 mm in size was scanned from 40 to 140°C. The heating rate of 2°C/min was selected. The scan amplitude and scanning frequency were 10 μm and 1.0 Hz, respectively.

The measurement of a JEOL JSM-6460LV scanning electron microscopy (SEM) was performed to observe phase separation of the blend films. The

blend film was immersed in liquid nitrogen before film fracture. The cryo-fractured films were sputter-coated with a thin layer of gold before measurement.

The tensile properties of blend films were determined with a LRX+ Lloyds Universal tensile machine at 25°C. The film samples (100 x 10 mm) were determined with an initial distance between the grips of 50 mm at an extension speed of 50 mm/minute. For each sample, five replicates were tested and average values were reported.

RESULTS AND DISCUSSION

Thermal transitions

The thermal transitions of scPLA/PBS blends including T_g, T_m and cold-crystallization temperature (T_{cc}) of PBS (PBS-T_m), homo-PLA (PLA-$T_{m,hc}$) and stereocomplex-PLA (PLA-$T_{m,sc}$) crystallites were measured from DSC curves as illustrated in Fig. 1. The Tg and Tcc of scPLA matrix decreased as increasing of the PBS ratios for both the blends without and with chain extender. This indicates the flexible PBS chains enhanced plasticizing effect in the amorphous regions of scPLA.[13] However, the T_g and T_{cc} of non-chain-extended blends were lower than the chain-extended blends. The results can be explain by the mobility of PLLA and PDLA chains were limited by branching structures of chain-extended blends.[21]

The PBS-T_m and PLA-$T_{m,sc}$ peaks of chain-extended blends slightly lower than the non-chain-extended blends. The branching structures also reduced crystal growth.[21] However, the PLA-$T_{m,hc}$ peaks of blends were nearly values in range 168-172°C.

The heat of cold crystallization (ΔH_{cc}) and heats of melting (ΔH_m) of PBS crystallites (PBS-ΔH_m), PLA homo-crystallites (PLA-$\Delta H_{m.hc}$) and PLA stereocomplex-crystallites (PLA-$\Delta H_{m.sc}$) obtained from DSC thermograms in Fig. 1 are summarized in Table 2. The ΔH_{cc} of blends decreased steadily as increasing the PBS ratios. This supports the PBS blending enhanced crystallization of the blends according to the literature.[16] The PBS-ΔH_m of the blends with and without chain extender increased as increasing the PBS contents. The PLA-$\Delta H_{m.hc}$ were in ranges 33.7–35.8 and 24.5–26.9 J/g for the blends without and with chain extender, respectively. The PBS-ΔH_m and PLA-$\Delta H_{m.hc}$ of the non-chain-extended blends were higher than the chain-extended blends. The results suggested the crystallization of both the PBS and homo-PLA crystallites was suppressed by chain extension. The PLA-$\Delta H_{m.sc}$ of the non-chain-extended blends steadily decreased while the chain-extended blends did not change (16.4°17.7) as the PBS ratios increased.

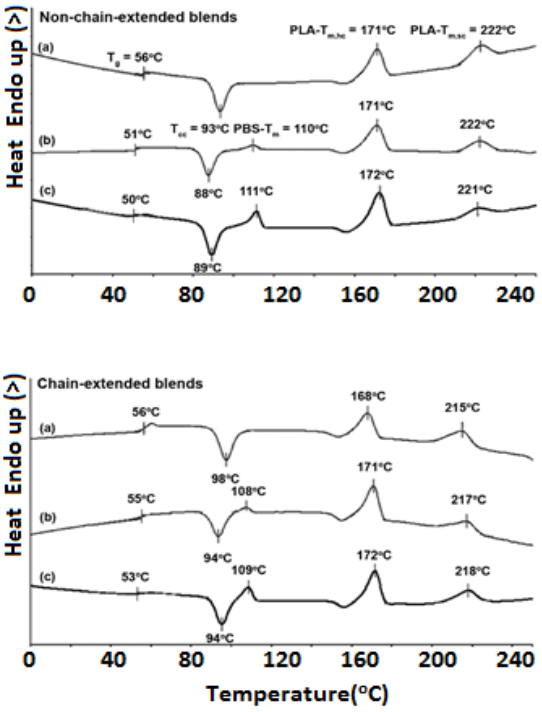

Fig. 1. DSC curves of blends (above) without and (below) with chain extender for scPLA/PBS weight ratios of (a) 100/0, (b) 95/5 and (c) 90/10

Table 2: DSC results of scPLA/PBS blends

scPLA/PBS (w/w)	DH_{cc} (J/g)	PBS-ΔH_m (J/g)	PLA-$\Delta H_{m.hc}$ (J/g)	PLA-$\Delta H_{m.sc}$ (J/g)
Non-chain-extended blends				
100/0	30.5	-	35.8	22.8
95/5	25.2	4.8	34.4	18.6
90/10	22.6	12.4	33.7	9.5
Chain-extended blends				
100/0	26.1	-	24.5	17.6
95/5	19.5	2.5	26.9	17.7
90/10	18	7.6	26.8	16.4

Thermal decompositions

Thermal decompositions of the scPLA/PBS blends were investigated from thermogravimetric (TG) thermograms (Fig. 2). Both the blend series

exhibited main thermal-decompositions in range 250–450^{O}C. The 90/10 scPLA/PBS blends with and without chain extender clearly showed thermal decompositions of PBS components as shoulder curves at higher temperatures. The PBS thermally-decomposed at higher temperature than the PLLA (data not shown). The non-chain-extended blends had slower thermal-decompositions than the chain-extended blends. These results were clearly observed from derivative TG (DTG) curves in Fig. 3. Temperatures of maximum decomposition-rate ($T_{d,max}$) peaks were shown.

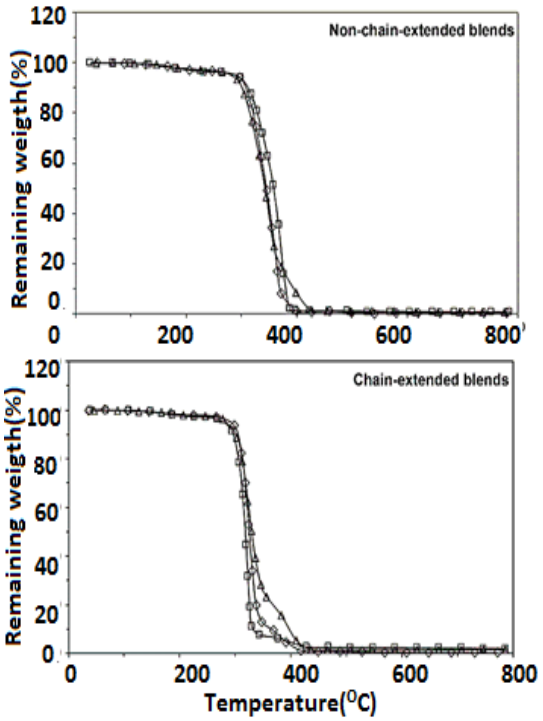

Fig. 2. TG curves of blends (above) without and (below) with chain extender for scPLA/PBS weight ratios of (□) 100/0, (♦) 95/5 and (Δ) 90/10

For the non-chain-extended blends, the $T_{d,max}$ peaks of scPLA and PBS components were in ranges 352–374^{O}C and 400–403^{O}C, respectively. The $T_{d,max}$ of scPLA matrix significantly moved to lower temperature when the PBS ratio was increased. The PBS chains penetrated between PLLA-PLLA, PDLA-PDLA and PLLA-PDLA chains to decreases their intermolecular interactions. The results indicate the scPLA/PBS blends were partially miscible. In addition the $T_{d,max}$ peaks of both scPLA and PBS components of the chain-extended blends were lower than the non-chain-extended blends. The branching structures of chain-extended blends suppressed intermolecular interactions of polymer chains.[17] It should be noted that the $T_{d,max}$ of scPLA matrix of chain-extended blends exhibited at higher temperature for the higher PBS content. The results indicated the chain extension could improve thermal stability of the scPLA matrix by chain extension with the higher thermal-stability PBS molecules.

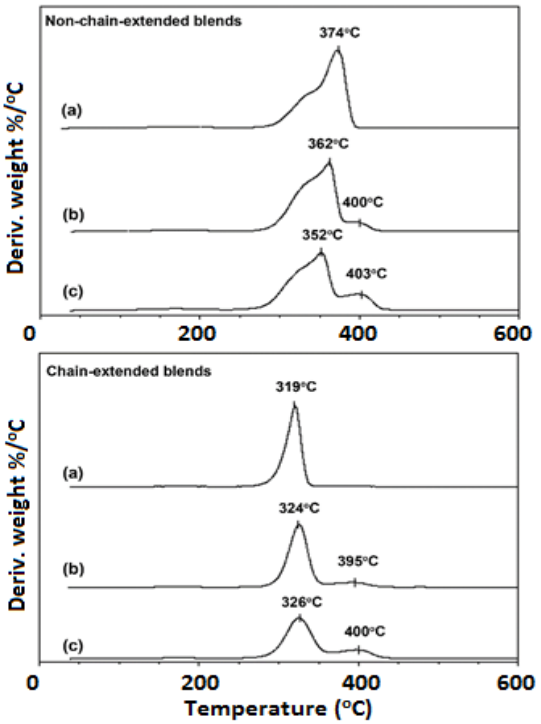

Fig. 3. DTG thermograms of blends (above) without and (below) with chain extender for scPLA/PBS weight ratios of (a) 100/0, (b) 95/5 and (c) 90/10. (Td,max peaks as shown)

Structures of blend crystallites

The XRD profiles of blend films were shown in Fig. 4 to investigate their crystalline structures. The 100/0 scPLA/PBS in Fig. 4 (above, a) showed only diffraction peaks at 12^{O}, 21^{O} and 24^{O} assigned to PLA stereocomplex crystallites.[22] It had no diffraction peaks of PLA homo-crystallites at 16.5^{O} and 19.0^{O}.[22] This result differs with previous DSC result in Fig. 1 (above, a) that the PLA-$T_{m,hc}$ peak was also observed. This may be explained by homo-PLLA and homo-PDLA crystallites of film matrix could have not formed during film forming by compression force at high temperature (T > PLA-$T_{m,hc}$).[23] In addition, the PLA homo-crystallization could be have occurred during DSC heating scan without external forces.[20] The 95/5 and 90/10 scPLA/PBS blend films exhibited

diffraction peaks at 19.7°, 22.0° and 29.3° attributed to PBS crystallites.[16] These peak intensities increased as the PBS ratios increased.

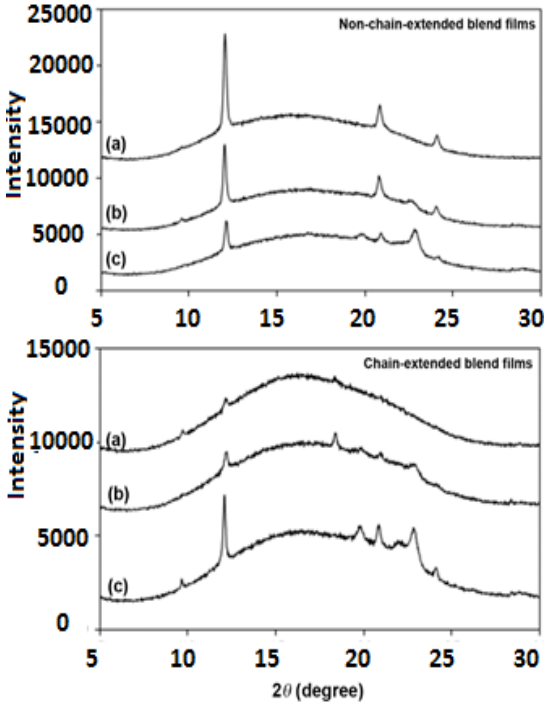

Fig. 4. XRD patterns of blend films (above) without and (below) with chain extender for scPLA/PBS weight ratios of (a) 100/0, (b) 95/5 and (c) 90/10

The PLA-$X_{c,sc}$ and PBS-X_c values are reported in Table 3. The PBS-X_c values increases with the PBS ratio for both the blend-film series. For the non-chain-extended blend films, the decreasing in PLA-$X_{c.sc}$ values was found when the PBS ratio was increased. This suggests the PBS blending inhibited stereocomplexation of non-chain-extended PLA matrix. The PLA-$X_{c.sc}$ values of scPLA film decreased from 9.2% to 0.7% when the scPLA was chain-extended. The stereocomplexation of PLA matrix was inhibited by branching structures of blend films with chain extension.20 The PLA-$X_{c.sc}$ of blend films with chain extension increased as the PBS ratio increased. The PBS could act as nucleating sites for PLA stereocomplexation. More free-volumes of branched structures of chain-extended blend films enhanced chain mobility for stereocomplex crystallization with PBS nucleating sites.

Thermo-mechanical properties

The thermo-mechanical properties from DMA analysis have been widely used to investigate heat-resistant property of PLLA and scPLA from changes of storage modulus and tan δ.[24–27] The storage modulus dramatically dropped in the region of glassy-to-rubbery transition for the poor heat-resistant PLLA due to its low X_c. After that, the storage modulus increases again during DMA heating because of PLLA cold-crystallization.[24] The PLLA with low X_c usually obtained from melt processes because of PLLA is slow crystallization rate. The annealed PLLA with high Xc maintained its stiffness on the T_g region to achieve its high heat-resistance.[27]

Table 3: Xc values of scPLA/PBS blend films from XRD

scPLA/PBS (w/w)	PLA-$X_{c.sc}$ (%)	PBS-X_c (%)
Non-chain-extended blends		
100/0	9.2	-
95/5	7.3	2
90/10	4.3	7.1
Chain-extended blends		
100/0	0.7	-
95/5	2.3	2.2
90/10	4.1	6.2

Figure 5 shows storage modulus of the scPLA/PBS blend films. The storage modulus of blend films without chain extender [Fig. 5 (above)] decreased from 4252-4536 MPa to 36-52 MPa when the temperature was increased up to 75°C before raising up during DMA heating. This indicates the heat resistance of non-chain-extended scPLA/PBS blend films did not change in significant by PBS blending. From Fig. 5 (below), the chain-extended scPLA film was largely dropped on storage modulus [see black line in Fig. 5 (below)]. This is due to the chain-extension reaction reduced the PLA-$X_{c,sc}$ of scPLA films from 9.2% to 0.7% as reported in Table 3. However, the storage modulus in the region of glassy-to-rubbery transition of chain-extended scPLA film was significantly improved by 5% and 10% PBS blending [see red and blue lines, respectively, in Fig. 5 (below)]. This is due to the PLA-$X_{c,sc}$ of chain-extended blend films were higher; 2.3% and 4.1% for 95/5 and 90/10 scPLA/PBS blend films, respectively. The results indicated that the stiffness and heat-resistant property of the chain-extended scPLA films can be improved by blending with PBS.

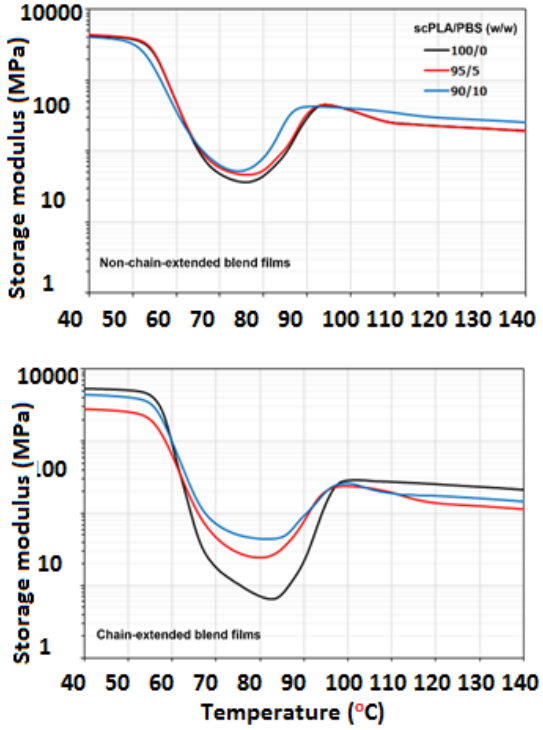

Fig. 5. Storage modulus from DMA of blend films (above) without and (below) with chain extender with various scPLA/PBS ratios

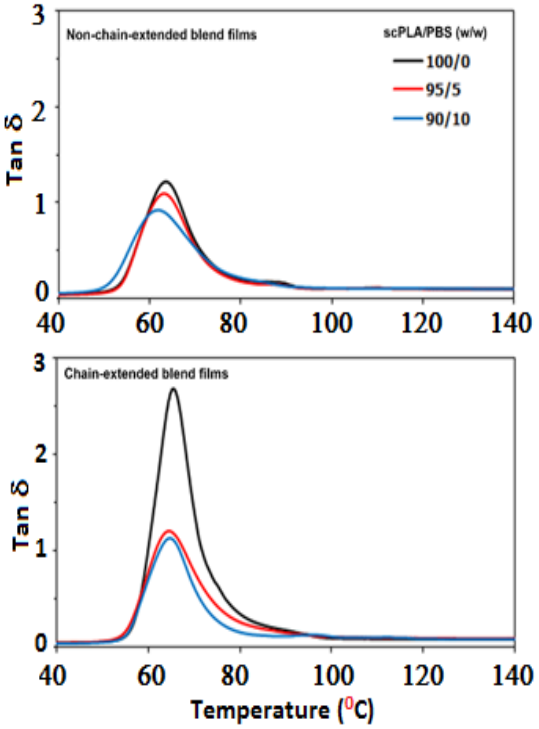

Fig. 6. Tan δ from DMA of blend films (above) without and (below) with chain extender with various scPLA/PBS ratios

The heat resistance of scPLA/PBS blend films was also elucidated from tan δ curves as shown in Fig. 6. The area of tan δ peak indicates the damping ability; the ability of samples to absorb and dissipate energy.[26,27] The areas underneath the tan δ peak of the blend films without chain extension for various scPLA/PBS ratios [Fig. 6 (above)] were similar suggested the heat resistance of these films was similar. For the blend films with chain extension, the area underneath the tan δ peak of the scPLA film [see black line in Fig. 6 (below)] was the largest. When 5% and 10% PBS were blended, the peak areas of the blend films significantly decreased [see red and blue lines, respectively, in Fig. 6 (below)]. The results indicated the chain mobility of scPLA matrix was restricted on the glassy-to-rubbery transition. Therefore the stiffness of chain-extended scPLA films was enhanced by PBS blending. It could be confirmed that the PBS blending enhanced stiffness and heat resistant properties of the chain-extended scPLA films.

Phase separation

Phase separation between continuous scPLA matrix and dispersed PBS phases was observed from film cross-sections as shown in Fig. 7. The PBS particles of all the blend films were nearly spherical in shape with good distribution. However, many voids were found for the non-chain-extended blend films with 5% and 10% PBS [Fig. 7 (left, b) and (left, c)]. This suggests poor phase-compatibility in the blend films.15 The de-bonded PBS particles may be removed out during film cryo-fraction. The blend films with chain extender presented fewer voids. Therefore chain extension enhanced phase compatibility of the scPLA/PBS blends. This could be explained by the molecules of chain-extended blends consisted of both PLA (PLLA and PDLA) and PBS chains. These molecules could act as compatibilizers to enhance phase adhesion of the scPLA/PBS blends.[14]

Tensile properties

Average tensile properties of the blend films were shown in Fig. 8. It was found that stress at break steadily reduced and strain at break slightly improved as increasing the PBS ratios. This is due

to the high flexibility of PBS.[16] The blend films with chain extension exhibited more stress and strain at break than without chain extension for the same scPLA/PBS blend ratio. The long-chain branching structures improved these tensile properties. However, the the PBS and chain extender did not change Young's modulus of the blend films.

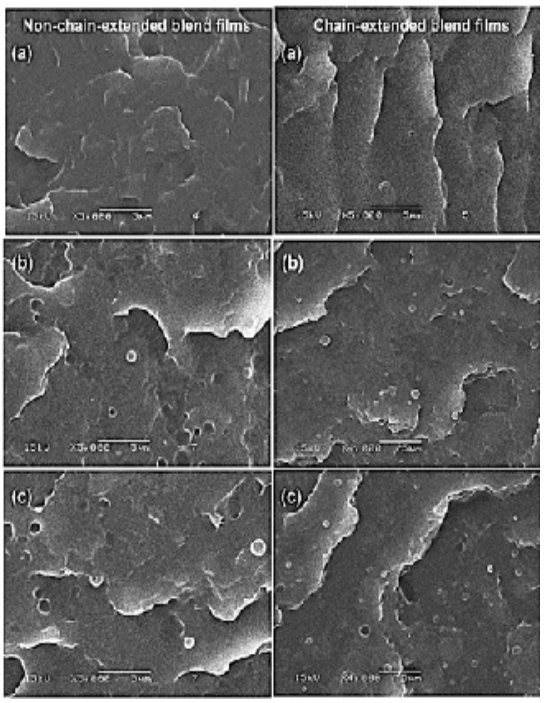

Fig. 7. SEM images of film cross-sections (left column) without and (right column) with chain extension for scPLA/PBS weight ratios of (a) 100/0, (b) 95/5 and (c) 90/10 (All bar scales = 5.0 μm)

CONCLUSION

The blends of scPLA/PBS without and with chain extender were prepared by melt blending. The PBS blending enhanced chain mobility of scPLA matrix in an amorphous phases to decreases its T_g and T_{cc}. However, both the T_g and T_{cc} of the blend films shifted to higher temperature by chain extension. The phase adhesion between scPLA matrix and dispersed

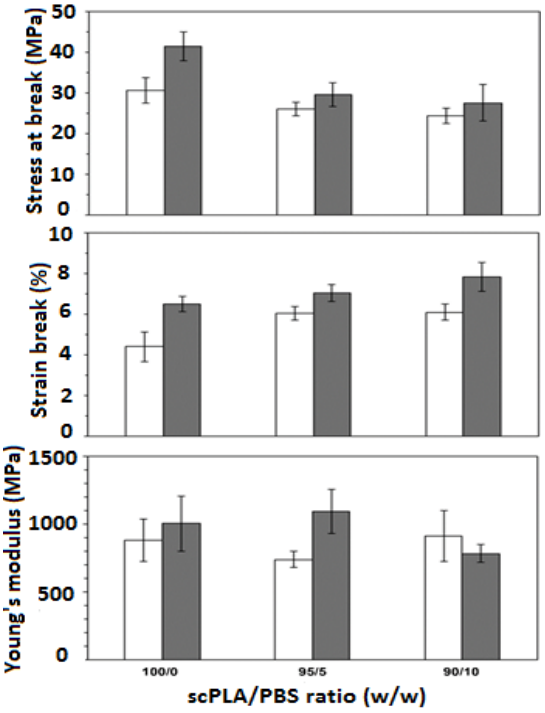

Fig. 8. Tensile properties of blend films (□) without and (■) with chain extender for scPLA/PBS weight ratios of (a) 100/0, (b) 95/5 and (c) 90/10

PBS particles could be improved by chain-extension reaction. The PBS blending improved the heat resistance of chain-extended scPLA films. Finally, chain extender enhanced film extensibility of blend blends. These results suggest that more flexible and good heat resistant scPLA/PBS blend films with chain extender can be used for development of high performance bioplastics.

ACKNOWLEDGEMENT

This research was funded by Mahasarakham University (grant no. 6105032).

Conflict of Interest

The authors declare that there is no conflict of interest.

REFERENCES

1. Rocca-Smith, J.R.; Whyte, O.; Brachais, C.; Champion, D.; Piasente, F.; Marcuzzo, E.; Sensidoni, A.; Debeaufort, F.; Karbowiak, T. *ACS Sustain. Chem. Eng.*, **2017**, *5*, 2715-2762.
2. Castro-Aguirre, E.; Auras, R.; Selke, S.; Rubino, M.; Marsh, T. *Polym. Degrad. Stab.*, **2018**, *154*, 46-54.
3. Silva, D.; Kaduri, M.; Poley, M.; Adir, O.; Krinsky, N.; Shainsky-Rotiman, J.; Schroeder, A. *Chem. Eng. J.*, **2018**, *340*, 9-14.

4. Nootsuwan, N.; Sukthavorn, K.; Wattanathana, W.; Jongrungruangchok, S.; Veranitisagul, C.; Koonsaeng, N.; Laobuthee, A. *Orient. J. Chem.*, **2018**, *34*(2), 683-692.
5. Yang, Y.; Zhang, L.; Xiong, Z.; Tnag, Z.; Zhang, R.; Zhu, *J. Sci. China Chem.*, **2016**, *59*(11), 1355-1368.
6. Tsuji, H. *Adv. Drug Deliv. Rev.*, **2016**, *107*, 97-135.
7. Cui, C.–H.; Yan, D.–X.; Pang, H.; Jia, L.–C.; Xu, X.; Yang, S.; Xu, J.–Z.; Li, Z.–M. *Chem. Eng. J.*, **2017**, *323*, 29-36.
8. Pasee, S.; Cheerarot, O.; Baimark, Y. *Orient. J. Chem.,* **2015**, *31*(3), 1551-1558.
9. Li, Y.; Xin, S.; Bian, Y.; Dong, Q.; Han, C.; Xu, K.; Dong, L. *RSC Adv.*, **2015**, *5*, 24352-24362.
10. Jiang, L.; Shen, T.; Xu, P.; Zhao, X.; Li, X.; Dong, W.; Ma, P.; Chen, M. *e-Polymers.,* **2016**, *16*(1), 1-13.
11. El-Khodary, E.; Fukui, Y.; Yamamoto, M.; Yamane, H. *J. Appl. Polym. Sci.*, **2017**, *134*, 45489.
12. Ojijo, V.; Ray, S.S.; Sadiku, R. *ACS Appl. Mater. Interfaces.*, **2013**, *5*, 4266-4276.
13. Pivsa-Art, W.; Fujii, K.; Nomura, K.; Aso, Y.; Ohara, H.; Yamane, H. *J. Appl. Polym. Sci.,* **2016**, *133*, 43044.
14. Salehiyan, R.; Ray, S.S.; Bandyopadhyay, J.; Ojijo V. *Polymers.,* **2017**, *9*, 350.
15. Fenni, S.E.; Monticelli, O.; Conzatti, L.; Doufnoune, R.; Stagnaro, P.; Naddaoui, N.; Cavallo, D. *Express Polymer Letters.,* **2018**, *12*(1), 58-70.
16. Zhang, X.; Liu, Q.; Shi, J.; Ye, H.; Zhou, Q. *J. Polym. Environ.*, **2018**, *26*, 1737-1744.
17. Baimark, Y.; Cheerarot, O. *Orient. J. Chem.*, **2015**, *31*(2), 635-641.
18. Murariu, M.; Paint, Y.; Murariu, O.; Raquez, J.-M.; Bonnaud, L.; Dubois, P. *J. Appl. Polym. Sci.*, **2015**, *132*, 42480.
19. Tuna, B.; Ozkoc, G. *J. Polym. Environ.*, **2017**, *25*, 983-993.
20. Baimark, Y.; Kittipoom, S. *Polymers.,* **2018**, *10*, 1218.
21. Chen, P.; Yu, K.; Wang, Y.; Wang, W.; Zhou, H.; Li, H.; Mi, J.; Wang, X. *J. Polym. Environ.*, **2018**, *26*, 3718-3730.
22. Lee, S.; Kimoto, M.; Tanaka, M.; Tsuji, H.; Nishino, T. *Polymer.,* **2018**, *138*, 124-131.
23. Pan, G.; Xu, H.; Ma, B.; Wizi, J.; Yang, Y. *J. Mater. Sci.*, **2018**, *53*, 5490-5500.
24. Vadori, R.; Mohanty, A.K.; Misra, M. *Macromol. Mater. Eng.*, **2013**, *298*, 981-990.
25. Nuzzo, A.; Coiai, S.; Carroccio, S.C.; Dintcheva, N.T.; Gambarotti, C.; Filippone, G. *Macromol. Mater. Eng.*, **2014**, *299*, 31-40.
26. Srithep, Y.; Pholharn, D.; Turng, L.-S.; Veang-in, O. *Polym. Degrad. Stab.*, **2015**, *120*, 290-299.
27. Zhang, X.; Meng, X.L.; Li, G.; Liang, N.; Zhang, J.; Zhu, Z.; Wang, R. *J. Appl. Polym. Sci.*, **2016**, *133*, 42999.